CrossMark

ORIGINAL ARTICLE

Characterisation and milling time optimisation of nanocrystalline aluminium powder for selective laser melting

Quanquan Han[1] · Rossitza Setchi[1] · Sam L. Evans[1]

Abstract The aim of this study is to investigate the properties of high-energy ball-milled nanocrystalline aluminium powders and to determine the optimum milling time required to produce an advanced aluminium powder for selective laser melting (SLM). Previous research has indicated that powders suitable for SLM include milled nanocrystalline aluminium powders with an average grain size of 60 nm and good flowability (Carr index less than 15 %). This study employs advanced nanometrology methods and analytical techniques to investigate the powder morphology, phase identification, average grain size and flowability of ball-milled powders. Stearic acid is used to prevent excessive cold welding of the ball-milled powder and to reduce abrasion of the grinding bowl and balls. The results indicate that, whilst the average particle size achieves a steady state after 14 h of milling, the grain size continues to decrease as the milling time progressed (e.g. the transmission electron microscopy measured average grain size is 56 nm after 20 h of milling compared to 75 nm for 14 h of milling). The aluminium powders milled for 16 and 20 h exhibit good flow behaviour, achieving a Carr index of 13.5 and 15.8 %, respectively. This study shows that advanced nanocrystalline aluminium powders suitable for SLM require ball milling for between 16 and 20 h, with 18 h being the optimum milling time.

Keywords High-energy ball milling · Nanocrystalline materials · Pure aluminium · Flowability · Selective laser melting

✉ Rossitza Setchi
  setchi@cf.ac.uk

[1] Cardiff University, Cardiff, UK

1 Introduction

Due to its light weight, high specific strength and good corrosion resistance, aluminium has found a wide range of applications in various domains, including the automotive and aerospace industries [1, 2]. However, fabricating customised and functional components with complex shapes is always a challenge when using traditional manufacturing technologies, e.g. casting, extrusion and computer numerical control (CNC) machining. Based on the layer-by-layer manufacturing principle, additive layer manufacturing (ALM) technology provides an integrated way of manufacturing three-dimensional (3D) complex-shaped components from computer-aided design (CAD) files, and it has become one of the most rapidly developing advanced manufacturing technologies in the world [3, 4]. Among the ALM techniques, selective laser melting (SLM) is being widely used to manufacture 3D complex-shaped metallic parts [5]. Therefore, the SLM of aluminium powders is expected to show great potential in the fabrication of advanced engineering components to meet the demanding requirements of the aerospace, automotive and biomedical industries.

Studies have shown that hot pressed parts manufactured using ultrafine nanocrystalline aluminium powders with an average grain size of 60 nm provide yield strength of 592 MPa [6]. Due to the superfast heating and cooling rate in SLM, the remaining nuclei of the nanocrystalline aluminium grains, together with the high nucleation rate, results in the formation of a fine microstructure in produced parts. The effect of grain refinement on the mechanical properties of aluminium and other metals and alloys (e.g. copper and titanium) has been investigated in the past [7]. It has been found that, compared to coarse grains, fine grains can provide more grain boundaries, which disrupt dislocation motion due to

the lack of slip plane and orientation, and further improve the yield strength of parts.

Therefore, it is crucial to produce advanced nanocrystalline aluminium powders with an average grain size of 60 nm for use in the SLM process. By comparison with other processes, the high-energy ball milling (also known as mechanical milling) process has proved to be a simple and effective technique to refine particle grain size and produce ultrafine grained (100 nm–1 μm) and nanocrystalline (~100 nm) materials for use in various domains [8–10]. Another advantage of high-energy ball milling lies in its ability to produce bulk quantities of solid-state materials using simple equipment at room temperature.

This paper explores the characteristics of advanced ball-milled nanocrystalline aluminium powders, including powder morphology, average grain size and powder flowability. An understanding of the powder characteristics is crucial for engineers to optimise the milling time to produce advanced aluminium powders suitable for SLM. Therefore, this paper has two objectives: first, to investigate the aluminium powder properties with respect to milling time and second, to determine the optimum milling time required to produce the SLM suitable aluminium powders with an average grain size of 60 nm and good flowability.

The remainder of this paper is structured as follows: in Sect. 2, a review of related work on high-energy ball milling is presented, highlighting the progress made in the ball milling of aluminium powders. Section 3 presents the materials and methods used in this study. The experiments results, together with the discussion, emphasising the average grain size and powder flow behaviour when optimising milling time, are presented in Sect. 4. Section 5 concludes with a summary of the main points and suggestions for further research.

2 Related work

The high-energy ball milling process was initially employed to produce oxide dispersion-strengthened (ODS) nickel and iron-based super alloys for use in aerospace industry [11]. After almost 40 years of development, the technique was shown to be capable of producing different types of advanced materials, including amorphous alloy powders, nanocrystalline powders and composite and nanocomposite powders [12].

Amongst the early studies of this technique, Lee and Koch [13] showed that amorphous powders can be produced via the high-energy ball milling of a mixture of two intermetallic compounds and, further, that the morphological development during the mechanical alloying of these powders is different from mechanical alloying using only pure ductile crystalline elemental powders. Rodriguez et al. [14] studied the structure and properties of attrition-milled aluminium powders and

found that aluminium powders milled for 10 h exhibited a Vickers microhardness (127 HV) of more than six times higher than the starting powder (20 HV). Cintas et al. [15] used vacuum attrition milling, cold pressing and vacuum pressing to produce nanocrystalline aluminium powders with an average grain size of 550 nm. Their study mainly focused on the influence of milling media on the microstructure of milled aluminium powders. High-strength aluminium has been produced by attrition milling in an ammonia gas atmosphere and powder consolidation by cold pressing and sintering. Indeed, a bulk sample with an average grain size of 200 nm exhibited a high tensile strength of 515 MPa and outstanding high-temperature behaviour [16].

More recently, Khan et al. [8] investigated the effect of grain refinement on the mechanical properties of ball-milled bulk aluminium and found that the strength increased from 35 MPa for coarse-grained material to 370 MPa for the sample with an average grain size of 75 nm following 20 h of milling. Choi et al. [17] studied the tensile behaviour of bulk nanocrystalline aluminium synthesised by the hot extrusion of ball-milled powders and ascertained that the aluminium powders milled for 48 h with an average grain size of 48 nm had a superior yield stress of 500 MPa with ductile fracture. The most interesting finding to date has been from Poirier and his colleagues; they investigated the yield strength of hot-pressed ball-milled aluminium powders and determined that milled pure aluminium powders with an average grain size of 60 nm had average yield strength of 592 MPa [6].

Previous studies focused mainly on the effect of milling speed, milling time or milling media on the grain refinement and mechanical strength of the components fabricated by traditional manufacturing processes (e.g. casting, extrusion); however, they have not considered both the gain size and flowability to determine the optimum milling time to produce advanced ball-milled aluminium powder suitable for SLM. This paper thereby investigates the characteristics of ball-milled nanocrystalline aluminium to determine the optimum milling time required to produce such aluminium powder with an average grain size of 60 nm and good flowability. In this work, four typical process parameters are studied, including milling speed, ball-to-powder weight ratio, process control agent (PCA) and milling time. Details of how the optimum parameters are chosen in this work are provided in the next section.

3 Materials and methods

Commercial pure aluminium powder (−325 mesh, 99.5 %) provided from Alfa Aesar was used in this study, and the particle size distribution was analysed with the Malvern Mastersizer3000. Figure 1 shows the morphology and particle
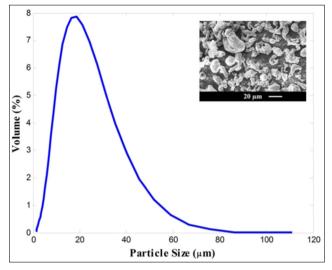
Fig. 1 Raw aluminium morphology and particle size distribution

size distribution of raw aluminium, with a measured average particle size of 17.1 μm.

The laboratory planetary mill (PULVERISETTE 5 classic line) was employed with four working stations to conduct the ball milling experiments. Generally, the typical process parameters of high-energy ball milling include milling speed, ball-to-powder weight ratio, PCA percentage and milling time. The milling speed is important because the faster the mill rotates, the higher would be the energy input into the powder; however, depending on the design of the mill, there are certain limitations to the maximum speed that can be used. The maximum milling speed of the employed laboratory planetary mill is up to 400 rpm, but the commissioning indicates that strong vibration can be generated when the milling speed is set at 400 rpm; the employed milling speed in this work thereby is set at 350 rpm.

The ball-to-powder weight ratio is another important variable in the milling process and has been varied from 1:1 to 10:1 while milling the powder in a small capacity mill. The capacity of the employed bowl is 500 ml, and the suggested sample volume should be between 80 and 225 ml to keep sufficient space for the motion of the grinding balls, and the ball-to-powder weight ratio is thereby determined to be 5:1. It has been proposed that the highest collision energy can be obtained if balls with different diameters are used [18]; therefore, stainless steel balls with two types of diameters (10 and 20 mm) were loaded to mill the aluminium powder in this work. To balance the weight, an equally heavy grinding bowl filled with sand was loaded symmetrically (Fig. 2a). Furthermore, to prevent oxidation during the high-energy ball milling process, the grinding bowl was filled with argon gas, and a lock device was used to gas-tight seal the bowl in the glove box, as shown in Fig. 2b.

A PCA, also known as lubricant, is added to the powder during the milling to reduce the effect of excessive cold welding. A wide range of PCAs has been used in practice at a level of about 1–5 wt.% of the total powder charge. The used PCA in this work is stearic acid and 3 wt.% of stearic acid has been widely used in previous studies when ball milling of aluminium powders; this is because 3 wt.% is sufficient to not only prevent excessive cold welding of the milled aluminium but also minimise the contamination of the ball-milled powders [16, 18]; therefore, the suggested 3 wt.% of stearic acid is employed and 200 g of aluminium powder without stearic acid was milled followed by 200 g of aluminium powder with 3 wt.% stearic acid in this work.

Milling time is considered to be the most important parameter in the high-energy ball milling process. Normally, insufficient milling time is unable to produce the milled powders with required characteristics (e.g. tiny grain size, spherical particle shape and good flowability); however, it should be noted that the level of contamination increases and some undesirable phases form if the powder is milled for times longer than required. Furthermore, a longer milling time contributes to consume more electricity energy. Therefore, it is desirable that the powder is milled just for the required duration and not any longer.

The milled aluminium samples were taken out every 2 h and subjected to analytical techniques for phase identification, purity measurement, grain size measurement and flow behaviour analysis and to determine microstructural changes. More specifically, scanning electron microscopy (SEM) was used to observe the powders' morphological evolution and transmission electron microscopy (TEM) was used to measure the average grain size of the ball-milled nanocrystalline powders. In addition, the average grain size was also evaluated by an X-ray diffraction (XRD) method when the grain size was less than 100 nm. The average grain size d can be expressed as [17]

$$d = \frac{0.9\lambda}{\beta \cos \theta} \tag{1}$$

Where β and θ denote the full width at half maximum (FWHM) and Bragg angle, respectively, and λ is the wavelength of the X-radiation. This formula is otherwise known as the Scherrer equation. In this study, XRD was also used to determine the phases formed during the milling process, and energy-dispersive X-ray spectroscopy (EDS) was used to measure the atomic and weight percentages of the constituent elements. To measure the milled powders' flow behaviour, the indicator of Carr index (CI) was used, which is the ratio of the difference between the tapped density and the apparent density to the tapped density, and can be expressed as [19, 20]

$$CI = \frac{\rho_T - \rho_A}{\rho_T} \times 100\% \tag{2}$$

where ρ_A denotes the apparent density, which results from pouring the powder into a heap or container in the absence of
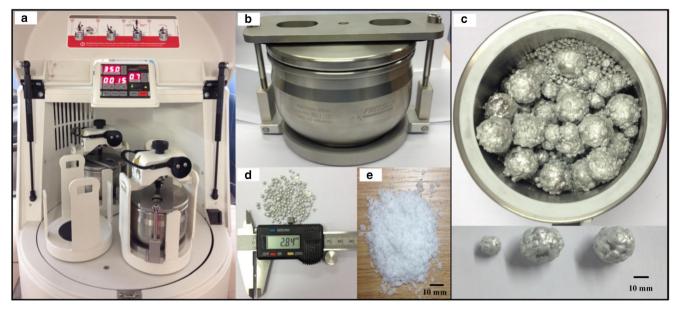
Fig. 2 The apparatus and milled aluminium powders without a PCA

any applied compression, and ρ_T represents the tapped density resulting from the application of compression, for example, impact or vibration. Generally, a Carr index of less than 15 % is considered to be an indicator of good flowability whilst greater than 20 % indicates poor flowability [21, 22]. The apparent and tapped densities of the aluminium powders in this study were measured according to ASTM D7481-09 to calculate the Carr index using a graduated cylinder.

4 Results and discussion

4.1 Morphological evolution

The milled aluminium powder without a PCA is shown in Fig. 2c up to 6 h of milling. It can be seen that the aluminium particles welded together to form a spherical shape with an average particle size of 2.5 mm (Fig. 2d). It should be noted that some of the particles stuck to the surface of the stainless steel balls and some were a platy shape. This can be attributed to the ductile and soft nature of aluminium. Unfortunately, the stuck ductile aluminium hindered further grain refinement due to a lack of sufficient collision energy. Figure 3 shows the aluminium particle size variation following up to 6 h of milling without a PCA. The average particle size remained approximately 2.5 mm after 2 h of milling, which verified the fact that the stuck aluminium hindered further grain refinement and confirmed the necessity for the usage of a lubricant. Therefore, 3 wt.% stearic acid (Fig. 2e) was added to refine the aluminium grain size to a nanoscale and avoid any unwarranted and excessive cold welding of the aluminium particles amongst themselves, onto the internal surface of the bowl and to the surfaces of the grinding balls.

SEM observation was conducted to investigate the morphological evolution of the aluminium powder during the ball milling process when stearic acid was added. Figure 4 shows the SEM micrographs of the milled aluminium as a function of the milling time. More specifically, Fig. 4a shows the morphology of the raw aluminium powder, which exhibited irregularly shaped particles with an average particle size of 17.1 μm. It can therefore be concluded that without the addition of a PCA, the irregularly shaped aluminium particles could have been converted to more spherical shapes (Fig. 2d) with an average particle size of 2.5 mm, but achieving a smaller particle size suitable for SLM would have been challenging.

When the aluminium powder was subjected to milling for 4 h, the particles deformed into flake-like shapes (Fig. 4b). This can be explained by the ductile nature of aluminium, plastic deformation and welding, which were the dominating mechanisms in this stage; this phenomenon was more prominent as the milling time increased to 8 h (Fig. 4c). With the
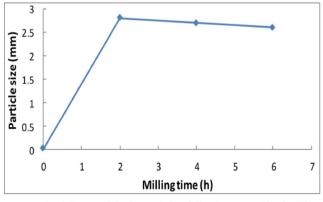

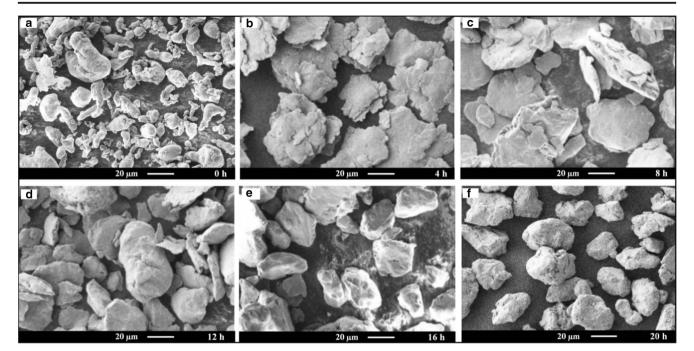**Fig. 3** Aluminium particle size variation following up to 6 h of milling

Fig. 4 The morphology of the aluminium powder ball milled for up to **a** 0, **b** 4, **c** 8, **d** 12, **e** 16 and **f** 20 h

continued milling process, the plate-like particles were subjected to work hardening and the fracture mechanism was activated, with the particle size tending to reduce with the extended milling time. Figure 4d shows the aluminium powder morphology subjected to 12 h of milling; some flake-like morphology remained amongst some aluminium particles, but many of the large flake-like particles tended to fracture, and some equiaxed aluminium particles formed. This phenomenon was more prominent as the milling time increased to over 12 h due to the fact that the flake-like particles were crushed by the intensive impacts generated by the grinding balls. After 16 h of milling, almost no flattened particles remained, and more aluminium particles exhibited equiaxed morphology with a narrow range of particle size distribution (Fig. 4e). Further milling up to 20 h had no significant effect on the powder morphology, as shown in Fig. 4f.

It can be concluded that the morphology of milled aluminium powder strongly depends on the milling time. In fact, the powder's morphological changes always lead to particle size and flow behaviour variations; cold welding tends to increase the particle size while fracturing results in a decrease in particle size.

To investigate the effect of milling time on particle size variation, SEM was used to measure the average particle size following up to 20 h of milling (Fig. 5). In the early stages, the average particle size can be considered to be linearly correlated with the milling time due to severe plastic deformation and the cold welding mechanism. The average particle size increased from the initial 17.1 to 51 μm following 10 h of milling. Subsequently, the fracture mechanism was activated, and the large aluminium particles were crushed by the intensive impacts, which led to a decrease in particle size. The measured average aluminium particle size at 20 h of milling was 33.1 μm compared to 32.8 μm at 14 h. It should be noted that the effect of the milling time had no significant effect on the average particle size of the ball-milled aluminium, and a relatively steady state was considered to be reached as the milling time exceeded 14 h. This can be explained by the fact that the dynamic balance between the cold welding and fracturing behaviours was reached after 14 h of milling, a finding that can aid the understanding of the optimum process parameters in the high-energy ball milling of pure aluminium powder.
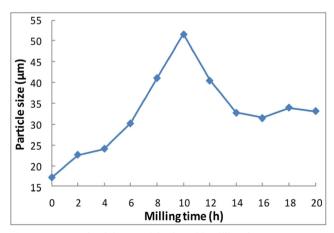

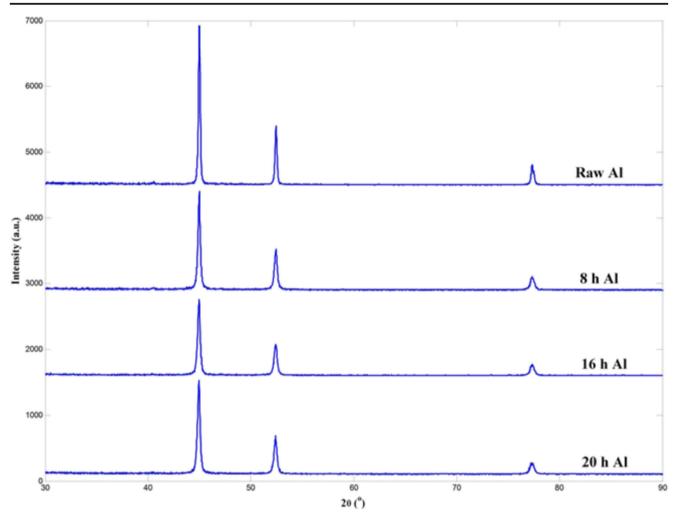**Fig. 5** Average aluminium particle size with milling time

Fig. 6 XRD patterns of the raw and ball-milled aluminium up to 20 h

4.2 Microstructural characterisation

To ascertain whether the high-energy ball milling process introduced any contamination into the milled aluminium powder, XRD and EDS were conducted to determine the phases that formed during the milling process. The XRD patterns of the raw and ball-milled aluminium powders were assessed using the PANalytical PW3830 X-ray generator with
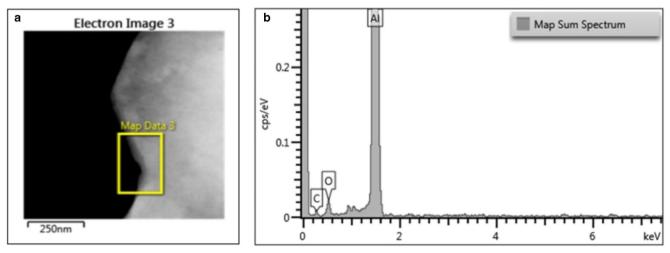

Fig. 7 EDS patterns of aluminium powder ball-milled for 20 h

Co K_α radiation ($\lambda = 0.1789$ nm) at 35 KV and 40 mA settings. The XRD patterns were recorded in the 2θ range of 30–90° using a continuous scan mode of 2.4°min^{-1}. Figure 6 shows the XRD patterns of the raw and ball-milled aluminium powders at different milling times. The diffraction patterns of the raw and ball-milled aluminium powders exhibited typical reflections for aluminium, which indicates that the iron elements from the grinding bowl and balls were not present or were below the levels of detection. This can be attributed to the fact that the added stearic acid acted as a surface-active agent and was absorbed on the surface of the grinding balls to reduce the wear of the stainless steel balls.

The weight percentage of the constituent elements of the milled powder was further investigated, and Fig. 7 shows the EDS spectra of the aluminium powder that had been ball milled for up to 20 h. The presence of the Al, C and O elements are evident from the peaks present in the spectrum, confirming that the milled aluminium powder did not accumulate any iron elements from the milling media (grinding bowl and balls). The atomic and weight fractions of these three elements are shown in Table 1. The presence of the C and O elements can be attributed to the addition of the 3 wt.% stearic acid and oxidation. It should be noted that, during the deposition stage in SLM, stearic acid acts as a lubricant and improves the flowability of nanocrystalline aluminium powder. On the other hand, in the laser melting stage, the added stearic acid could volatilise because the laser beam induces extremely high temperatures on the powder bed.

During the ball milling process, the grain size was effectively reduced due to the intensive impacts of the grinding media. The XRD patterns shown in Fig. 6 can also be used to evaluate the average grain size of the milled nanocrystalline aluminium powder. Three peaks can be observed at $2\theta = 44.98$, 52.43 and 77.33°, and all the patterns exhibited typical reflections for aluminium; however, compared to the patterns of the raw aluminium, the milled powder showed a broadened intensity, which means that the grain size was effectively reduced after milling. The FWHM of the diffraction patterns at 44.98° were 0.2362, 0.2952 and 0.3149 for aluminium powder ball-milled 8, 16 and 20 h, respectively. Equation (1) was used to evaluate the average grain size of the aluminium powder between 8 and 20 h of milling, and the determined values are shown in Fig. 8. It can be seen that the average grain size reduced from 71 to 48 nm as the milling time increased from 8 to 20 h.

To confirm the evaluated average grain size obtained by XRD, TEM observations were conducted. Figure 9 shows the TEM micrographs of the ball-milled aluminium powder after different milling times. More specifically, whilst the aluminium powder was subjected to 8 h of milling, the localisation of the plastic deformation in the form of shear bands contained a high density of dislocations; the intensive impacts from the grinding balls drove grain rotation and

Table 1 Atomic and weight fractions of the elements of aluminium ball-milled for 20 h

Element	Atomic %	Weight %
Al	89.13	94.39
C	7.74	3.65
O	3.13	1.96
Total	100	100

subgrain boundary sliding, which led to grain refinement with a measured average grain size of 137 nm. As the milling process continued, the dislocations continued to accumulate, and more new grains formed, leading to the measured average grain size reducing from 137 to 56 nm as the milling time increased from 8 to 20 h. It can be concluded that, whilst the average particle size of the milled aluminium powder remained steady after 14 hours of milling, the measured average grain size continued to reduce as the milling continued.

The TEM-measured average grain size with respect to milling time is shown in Fig. 8. The TEM-measured grain size results showed a similar trend to the XRD results, excluding the grain size value at 8 h of milling. The TEM-measured average grain size was 137 nm for aluminium powder milled for 8 h, compared to a value of 71 nm obtained using the Scherrer equation. It should be noted that the Scherrer equation could only be used to evaluate the average grain size when the grain size was less than 100 nm due to the fact that the TEM-measured grain size at 8 h was 137 nm, which indicates that the equation is not suitable for the calculation of grain size until 8 h of milling has been exceeded. Nevertheless, when the milling time was greater than 12 h, the average grain size assessed using Eq. (1) from the XRD patterns could be considered to be in agreement with the TEM-measured grain size and served to verify the grain size obtained by the TEM observations.

Due to the oxidation, a thin oxide film (3–5 nm) is generally formed on the surface of the ball-milled aluminium powder, which is considered to be one of the challenges in the
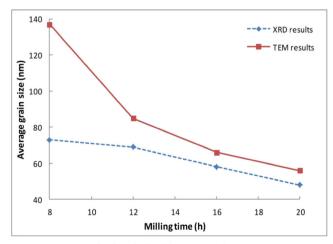

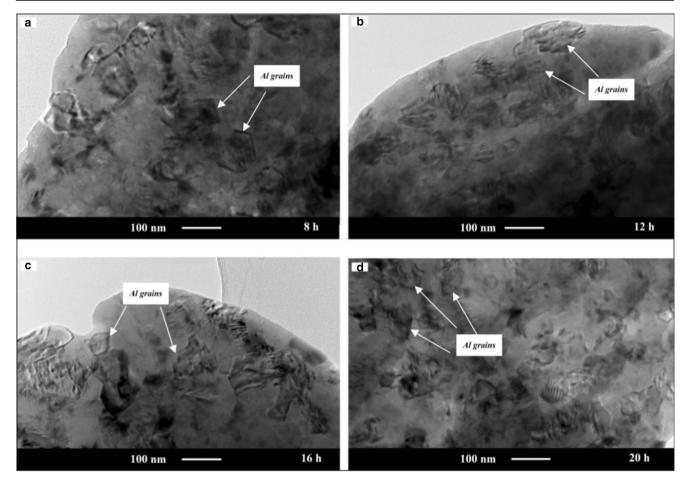**Fig. 8** Average grain size obtained by XRD and TEM

Fig. 9 TEM images of ball-milled aluminium powder subjected to **a** 8, **b** 12, **c** 16 and **d** 20 h of milling

SLM of aluminium powders, compared to SLM of other metal powders. The oxide film with a thickness of 3 nm was also observed in the milled aluminium powder using TEM and shown in Fig. 10; the marked dash line is the boundary between the aluminium particulate and formed oxide film. Due to the melting point depression, the melting point of the formed oxide film is generally decreased to about 1600 °C, which is much lower than the bulk alumina (2050 °C). An understanding of this is crucial for engineers to optimise the
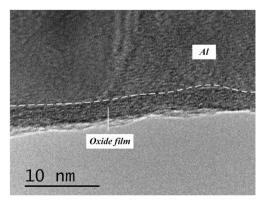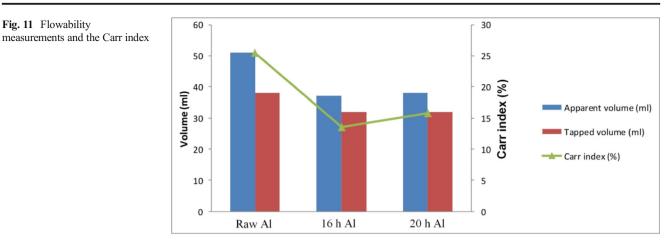

Fig. 10 Formed oxide film on the aluminium surface

process parameters in SLM to melt the oxide film during the track scanning, because the unmelted oxide films lead to the formation of pores in the subsequent solidification stage and further reduce the mechanical properties of the final parts.

4.3 Flow ability analysis

A powder's flowability behaviour is considered to be crucial in the SLM process as it determines the powder's deposition performance. Generally, good-flowing powders generate powder layers with continuous and uniform thickness while poor-flowing powders lead to non-uniform powder layers, which may influence the dimensional accuracy and mechanical properties of the final parts. The Carr index can be used to evaluate the flow behaviour of ball-milled aluminium powder. Powders with a Carr index of less than 15 % are considered to have good flowability while a Carr index greater than 20 % implies poor flowability.

Figure 11 shows the measurement results for 55 g of raw aluminium powder and the same mass of aluminium powder after 16 and 20 h of milling. The measured apparent and tapped volumes for the raw aluminium powder were 51 and 38 ml, respectively. The tapped

Fig. 11 Flowability measurements and the Carr index

volume was obtained by tapping the 100-ml cylinder 500 times and measuring the tapped volume to the nearest graduated unit. The density was calculated by the ratio of mass to the measured volume. Using Eq. (2), the Carr index was determined to be 25.5 %. Likewise, the measurements of the aluminium powder milled for 16 and 20 h were taken. The Carr index values for the aluminium powder milled for 16 and 20 h were determined to be 13.5 and 15.8 %, respectively. It can be concluded that the raw aluminium powder exhibited poor flowability with a Carr index of 25.5 %, which indicates that, during the deposition stage, a non-uniform powder layer may be generated during SLM. Therefore, the raw aluminium was considered to be unsuitable for SLM technology if no further processes were to be employed; however, the aluminium powder subjected to 16 h of milling exhibited good flow behaviour with a Carr index of 13.5 %. This can be explained by two main factors: the appropriate addition of stearic acid, which acted as a lubricant to improve the powder's flowability, and the changes in the powder's morphology. Compared to the irregular shape of the raw aluminium powder, the equiaxed powder morphology showed better flow behaviour. The obtained Carr index of 15.8 % implied that the aluminium powder milled for 20 h exhibited good flow behaviour as well, and this can be explained again by the addition of stearic acid and the powder's morphological changes.

It should be noted that the milling time had no significant effect on the Carr index once the milling time exceeded 16 h, which suggests that milled aluminium powder could exhibit good flow behaviour if the milling time is longer than 16 h. Therefore, if high-energy ball milling is used to produce advanced nanocrystalline aluminium powder for SLM, both the flowability of the milled powder and the obtained average grain size should be considered when determining the optimum milling time.

5 Conclusions and future research

This study employed the advanced nanometrology methods and analytical techniques to investigate the characteristics of the ball-milled nanocrystalline aluminium powder for the SLM process and determined the optimum milling time by considering the average grain size and flowability. The following important findings derived from the results were presented in this paper:

1. A PCA (e.g. stearic acid) proved to be necessary during the ball milling of the aluminium powder as it prevented excessive cold welding and contributed to the synthesis of the nanocrystalline aluminium powder.
2. During the early stages of ball milling, the average particle size increased concomitantly with the milling time; this is thought to be plastic deformation and cold welding. The measured maximum average particle size was 52 μm for 10 h of milling compared to 17.1 μm of the raw aluminium, and there is no other mechanism for the particle size to increase. Thereafter, the measured average particle size tended to reduce due to the fracture mechanism, and the average particle size achieved a steady state after 14 h of milling with a value of 32.8 μm.
3. Whilst the average particle size achieved a steady state after 14 h of milling, the grain size continued to decrease and this is thought to be dislocation accumulation and the formation of subgrain boundaries, as shown in the TEM images (Fig. 9). The TEM-measured average grain size declined from 77 nm following 14 h of milling to 56 nm at 20 h of milling, which was also confirmed by XRD (Fig. 8).
4. In terms of the XRD and EDS results, the aluminium milled for 20 h was not contaminated by iron elements from the grinding bowl and balls, which can be attributed to the appropriate addition of a PCA.
5. Both the aluminium powder milled for 16 and 20 h exhibited good flow behaviour, with a Carr index of 13.5

and 15.8 %, respectively. Therefore, to obtain an advanced nanocrystalline aluminium powder suitable for SLM with an average grain size of 60 nm and good flowability, the ball milling time should be between 16 and 20 h, with 18 h recommended as the optimum milling time.

This study explored the morphological and microstructural changes of ball milled-aluminium powders subjected to different milling times. The optimum milling time was consequently determined by considering both the average grain size and powder flowability. Nonetheless, the limitations of this study offer interesting directions for future studies. First, the average grain size was obtained by limited TEM-measured samples, which constrained the accuracy of the grain size evaluation. Second, whilst the optimum ball milling time of 18 h is recommended, its validity needs to be further verified, and the mechanical properties of SLM-produced parts need to be investigated to a greater extent. Lastly, to obtain a better understanding of the high-energy ball milling of advanced aluminium powders suitable for the SLM process, material suppliers, machine manufactures and academic researchers should ideally work together to provide a feasible solution.

References

1. Thijs L, Kempen K, Kruth JP, Van-Humbeeck J (2013) Fine-structured aluminium products with controllable texture by selective laser melting of pre-alloyed AlSi10Mg powder. Acta Mater 61:1809–1819
2. Ibrahim IA, Mohamed FA, Lavernia EJ (1991) Particulate reinforced metal matrix composites—a review. J Mater Sci 26:1137–1156
3. Patil RB, Yadava V (2007) Finite element analysis of temperature distribution in single metallic powder layer during metal laser sintering. Int J Mach Tools Manuf 47:1069–1080
4. Soe SP, Eyers DR, Setchi R (2013) Assessment of non-uniform shrinkage in the laser sintering of polymer materials. Int J Adv Manuf Technol 68(1):111–125
5. Gu DD, Meiners W, Wissenbach K, Poprawe R (2012) Laser additive manufacturing of metallic components: materials, processes and mechanisms. Int Mater Rev 57:133–164
6. Poirier D, Drew RAL, Trudeau ML, Gauvin R (2010) Fabrication and properties of mechanically milled alumina/aluminum nano-composites. Mater Sci Eng A 527:7605–7614
7. Padmanabhan KA (2001) Mechanical properties of nanostructured materials. Mater Sci Eng A 304–306:200–205
8. Khan AS, Farrokh B, Takacs L (2008) Effect of grain refinement on mechanical properties of ball-milled bulk aluminum. Mater Sci Eng A 489:77–84
9. Razavi-Tousi SS, Yazdani-Rad R, Salahi E, Mobasherpour I, Razavi M (2009) Production of Al-20wt.% Al2O3 composite powder using high energy milling. Powder Technol 192:346–351
10. Liao JZ, Tan MJ (2011) Mixing of carbon nanotubes (CNTs) and aluminium powder for powder metallurgy use. Powder Technol 208:42–48
11. Benjamin JS (1970) Dispersion strengthened superalloys by mechanical alloying. Metall Trans 1:2943–2951
12. Zhang DL (2004) Processing of advanced materials using high-energy mechanical milling. Prog Mater Sci 49:537–560
13. Lee PY, Koch CC (1988) Formation of amorphous Ni-Zr alloy powder by mechanical alloying of intermetallic powder mixtures and mixtures of nickel or zirconium with intermetallics. J Mater Sci 23:2837–2845
14. Rodríguez JA, Gallardo JM, Herrera EJ (1997) Structure and properties of attrition-milled aluminium powder. J Mater Sci 32:3535–3539
15. Cintas J, Montes JM, Cuevas FG, Herrera EJ (2005) Influence of milling media on the microstructure and mechanical properties of mechanically milled and sintered aluminium. J Mater Sci 40:3911–3915
16. Cintas J, Cuevas FG, Montes JM, Herrera EJ (2005) High-strength PM aluminium by milling in ammonia gas and sintering. Scr Mater 53:1165–1170
17. Choi HJ, Lee SW, Park JS, Bae DH (2008) Tensile behavior of bulk nanocrystalline aluminum synthesized by hot extrusion of ball-milled powders. Scr Mater 59:1123–1126
18. Suryanarayana C (2001) Mechanical alloying and milling. Prog Mater Sci 46:1–184
19. Carr RL (1965) Classifying flow properties of solids. Chem Eng 72:69–72
20. Cain J (2002) Flowability testing—an alternative technique for determining ANSI/CEMA standard 550 flowability ratings for granular materials. Powder Handl Process 14:218–220
21. Han Q, Setchi R, Evans SL (2016) Synthesis and characterisation of advanced ball-milled Al-Al2O3 nanocomposites for selective laser melting. Powder Technol. doi:10.1016/j.powtec.2016.04.015
22. Yadroitsev I (2009) Selective laser melting: direct manufacturing of 3D-objects by selective laser melting of metal powders. Lambert Academic Publishing, Saarbrucken